Supplementary Information

Understanding the stability and structural properties of Ordered Nanoporous Metals towards their rational synthesis

Jose M. Ortiz-Roldan,[1#] Salvador R. G. Balestra,[1,2#] Rocio Bueno-Perez,[3] Sofía Calero,[1,4] Elena Garcia-Perez,[a] C. Richard A. Catlow,[5,6,7]* A. Rabdel Ruiz-Salvador,[1]* Said Hamad[1]*

1. Department of Physical, Chemical and Natural Systems, University Pablo de Olavide, Ctra. Utrera km. 1, 41013, Seville, Spain.
2. [b.] Instituto de Ciencia de Materiales de Madrid (ICMM), Consejo Superior de Investigaciones Científicas (CSIC), c/ Sor Juana Inés de la Cruz 3, 28049, Madrid, Spain
3. [c.] Adsorption & Advanced Materials Laboratory (A2ML), Department of Chemical Engineering & Biotechnology, University of Cambridge, Philippa Fawcett Drive, Cambridge CB3 0AS, UK.
4. [d.] Materials Simulation and Modelling, Department of Applied Physics, Eindhoven University of Technology, 5600MB Eindhoven, The Netherlands
5. [e.] Department of Chemistry, University College London, 20 Gordon St., London WC1H OAJ, UK.
6. [f.] UK Catalysis Hub, Research Complex at Harwell, STFC Rutherford Appleton Laboratory, Chilton, Oxon, OX11 0FA, UK.
7. School of Chemistry, Cardiff University, Cardiff, CF10 1AT, UK.

[#] These authors equally contributed to this work

Email: S.H said@upo.es; ARR-S rruisal@upo.es and CRAC c.r.a.catlow@ucl.ac.uk

Contents

Section S1. EAM Potentials

Interatomic potentials of the Embedded Atom Method (EAM) were used, since their many-body nature allows a well-balanced description of metallic systems.[S1,S2] The energy of the system is described by:

$$E_{Total} = \frac{1}{2}\sum_{i,j}\phi_{ij}(r_{ij}) + \sum_{i,j}F_i(\rho_i) \qquad \text{Equation S1}$$

$$\rho_i = \sum_{j\neq i}\Psi_{ij}(r_{ij}) \qquad \text{Equation S2}$$

Where $\boldsymbol{\phi_{ij}(r_{ij})}$ are two-body terms and $\boldsymbol{F_i(\rho_i)}$ are many-body terms that depend on the electron density of the metallic system. The electron density is computed as the sum of the contribution of atoms within a given cutoff. In the Sheng et al. EAM potentials used in this work the above functions are fitted to ab-initio calculations using numerical quintic spline functions.[S3] The authors says that the "longdistance description" might be a surrogate for the "angular description." Note that this allows modelling of nanostructures with atomic environment apart of those found in bulk energy minima configurations. In addition, to allow large transferability for the construction of the potential energy surfaces used in the potential parameterization a variety properties of the elements were considered, including lattice dynamics, mechanical properties, thermal behavior, energetics of competing crystal structures, defects, deformation paths, liquid structures, and so forth.

The Ni and Pt potentials by Ortiz-Roldan et al.[S4] and Johnson,[S5] respectively, use Johnson's analytical description,[S5] of the type:

$$\phi_{ij}(r_{ij}) = Ae^{r_{ij}/d} - \frac{C}{r^6} \qquad \text{Equation S3}$$

$$F_i(\rho_i) = -\sum_{i,j}E_c\left[1 - \ln\left(\rho_i/\rho_{0_i}\right)^{\alpha_J/\beta}\right]\left(\rho_i/\rho_{0_i}\right)^{\alpha_J/\beta} + F_1\left(\rho_i/\rho_{0_i}\right)^{\gamma/\beta} \qquad \text{Equation S4}$$

$$\rho_i = \sum_{i,j}A_d e^{B_d(r_{ij}-r_0)} \qquad \text{Equation S5}$$

Where E_c is the cohesive energy, $\alpha_J = 3(\Omega B/E_c)$, (with Ω as the volume per atom, and B as the bulk modulus) and r_0 is the first nearest neighbour distance, $a/\sqrt{2}$ for an fcc metal where a is the lattice parameter.

All potentials used to model OMNs and bulk metals are supplied to the LAMMPS code as numerical tables, which are supplied here in separated files.

The files corresponding to the system xylene Ag-CRI-ST3 ONM are supplied as an example.

Section S2. Lattice energy and cell parameter time dependence for Pt-CRI-ST3

To show the stability of the ONMs, the lattice energy and cell parameter time dependence that we computed by MD simulations are plotted for Pt-CRI-ST3 ONM. Note that the energy variation is much smaller than the thermal energy (kT = 25 meV at 300K).

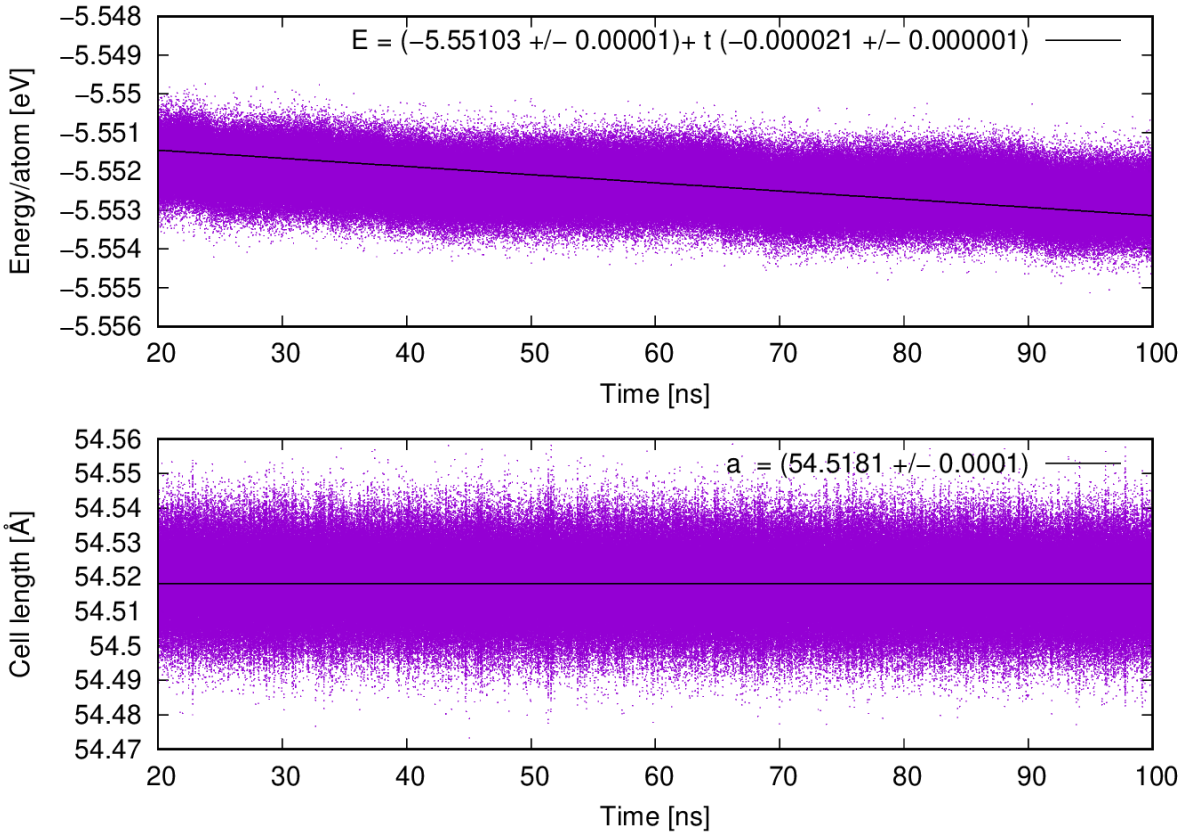

Figure S1. Lattice energy and cell parameter time dependence for Pt-CRI-ST3 ONM at 300 K.

Section S3. NVT stability of Ni-CRI-ST3 ONM

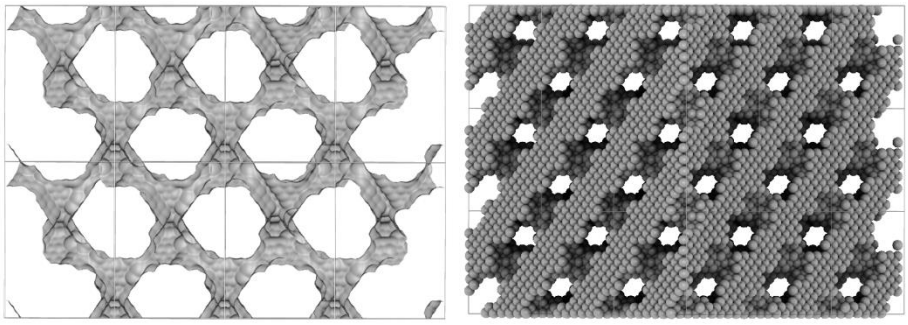

Figure S2: Atomistic views of the Ni-CRI-ST3 at 1000 K as modelled by NVT MD simulation.

We also obtained, however, that this structure collapses at 900 K when modelled with the more realistic NPT MD simulations and thus providing evidence of the inappropriateness of using NVT for studying the stability of hypothetical nanoporous solids.

Section S4. Metadynamics simulations

We have used the MetaD technique, using the flexible Gaussian approach (activated by the ADAPTIVE=GEOM keyword),[S6,S7] by exploiting the facilities provided by with the code PLUMED.[S8-S10] The choice of the metadynamics specific values has been made according to the characteristics of the system (see Code S1): SIGMA=0.1 Å and HEIGHT=1.2 kJ/mol, which is ~ $k_BT/2$. In addition to the metadynamics associated with the movement of the central atom of the referenced *nest*, we have also added a geometric constraint to the movement of the *nest* itself (by adding harmonic restraints on the geometrical variables which define the *nest*), so that when the central atom leaves, the *nest* does not lose its self-stability and ceases to exist as such, losing the reference for the moving atom and making it impossible for it to return.

As can be seen in Figure S1, the central atom leaves the nest and reaches a maximum distance of 12 Å(a limit imposed in the simulations) to return to the *nest* and repeat the process many times (note the time window from 1 ns to 3 ns) and thus calculate the free energy value of this process. The bias value (green line) is used to check that the MetaD is working correctly.

All three metals studied show a second minimum at distances less than a certain value. In order to reduce the error in the calculation of free energy barriers, in a second batch of simulations we have restricted the maximum distance to this distance, 5.5 Å. Thus, the moving atom scans the environment of the local equilibrium minimum efficiently for all compositions and environments. We have also used the multiple walker enhanced sampling technique (MULTIPLE_WALKERS keyword, in Code S1), in order to improve the efficiency of the exploration of the surface (see Figure S3). Error bars were calculated following the PLUMED tutorial and using some Python programs from the Masterclass (https://www.plumed.org/doc-master/user-doc/html/masterclass-21-2.html, and see Code S2).

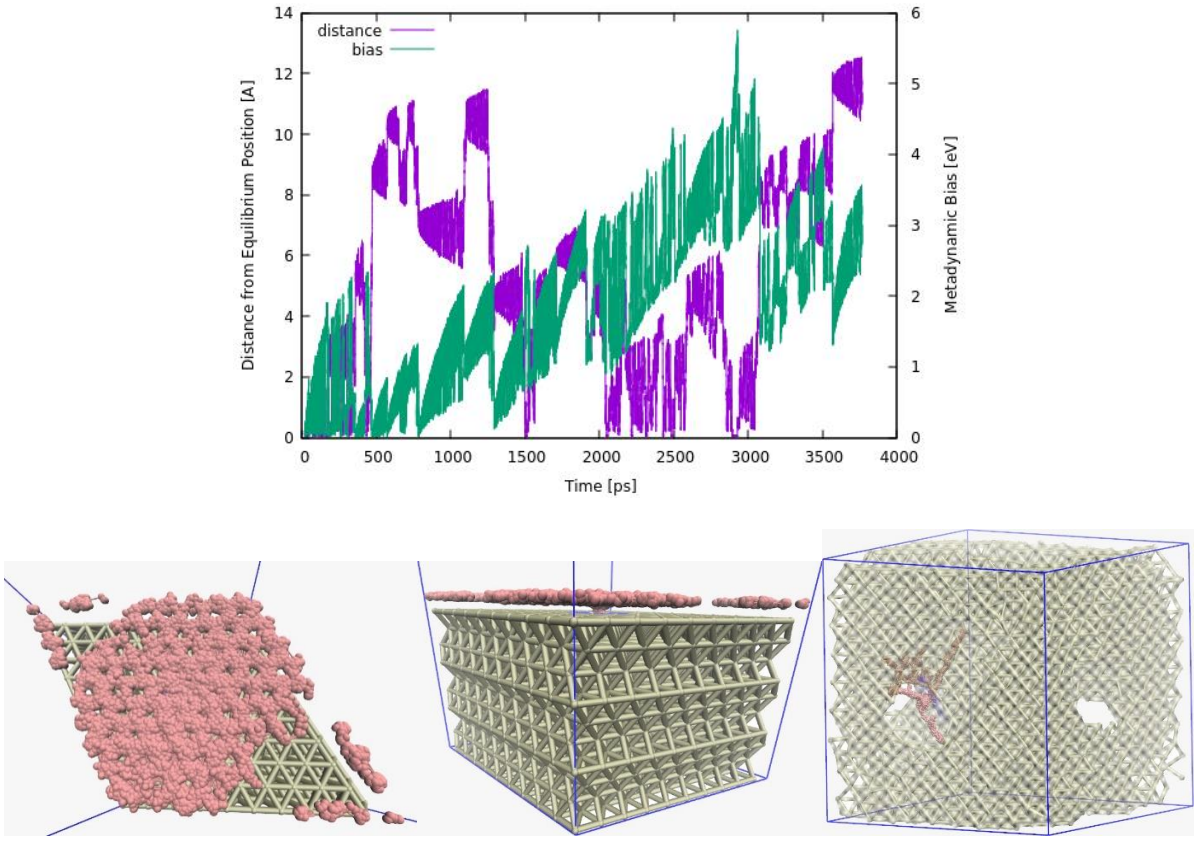

Figure S3: (Top) Evolution of the distance between an atom on the ONM surface and the centre of the defined cavity (a planar-like environment) over time (purple line). It can be observed that the atom goes in and out of the cavity or *nest*, allowing the free energy of the potential barrier to be calculated. The potential bias of the MetaD is also monitored (green line). **(Bottom Left and Middle)** Snapshot of the Ni surface (yellow atoms) and the superpositions of the trajectory of the moving Ni atom of the surface (pink spheres). **(Bottom Right)** Idem for ONM system. In this last snapshot we only superpose the last 100 ps, for clarity reasons.

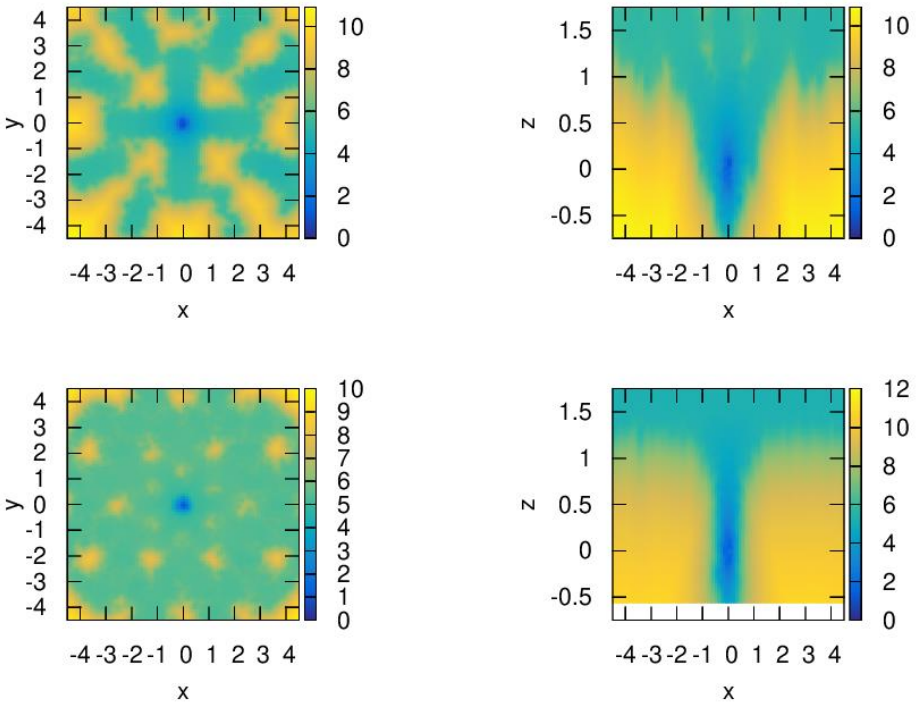

Figure S4: Free energy profiles (*xy* and *xz*-views) of the moving Ni atom on the (**Top**) 100 surface, and (**Bottom**) 111 surface. Energy and length units in eV and Å, respectively.

Code S1: Plumed code used in the MetaD simulation

```
#vim:ft=plumed
# Fix the "Pt-nest" atoms:
nest: CENTER ATOMS=102,110,1429,1508,2131,2201
d_1: DISTANCE ATOMS=nest,102
d_2: DISTANCE ATOMS=nest,110
d_3: DISTANCE ATOMS=nest,1429
d_4: DISTANCE ATOMS=nest,1508
d_5: DISTANCE ATOMS=nest,2131
d_6: DISTANCE ATOMS=nest,2201
# Restricted movement of the atoms of the Pt-nest to avoid the destruction of the nest.
res: COMBINE …
 ARG=d_1,d_2,d_3,d_4,d_5,d_6 POWERS=2,2,2,2,2,2  COEFFICIENTS=0.5,0.5,0.5,0.5,0.5,0.5
 PARAMETERS=0.274141,0.279685,0.277538,0.275844,0.267271,0.268732 PERIODIC=NO
…
# Surfer atom:
#ATOM    806  Au  MOL     0       4.870  18.200  25.710  1.00  0.00
# Move the surfer atom, define the distance "dd" between the surfer atom and the "nest":
dd:  DISTANCE ATOMS=nest,806
# Metadynamic input and Bias (length unit in nm, energy unit in kJ/mol)
mt: METAD …
ARG=dd SIGMA=0.01 HEIGHT=1.2 PACE=2500
 ADAPTIVE=GEOM SIGMA_MIN=0.001 SIGMA_MAX=0.1
 GRID_MIN=-0.05 GRID_MAX=0.55 GRID_BIN=250
 MULTIPLE_WALKERS
…
lwall: LOWER_WALLS ARG=dd AT=0.01 KAPPA=5000 EXP=2
uwall: UPPER_WALLS ARG=dd,res AT=1.0,0.0005 KAPPA=5000,5000000 EXP=2,2
bias:  COMBINE ARG=*.bias PERIODIC=NO
PRINT STRIDE=100 ARG=* FILE=COLVAR_all
PRINT STRIDE=100 ARG=dd,bias FILE=COLVAR
FLUSH STRIDE=100
ENDPLUMED
```

Code S2: Reweighting and calculating the histograms

```
#vim:ft=plumed
nest: CENTER ATOMS=102,110,1429,1508,2131,2201
dd:  DISTANCE ATOMS=nest,806
mt: METAD ...
 ARG=dd SIGMA=0.01 HEIGHT=1.2 PACE=2500
 ADAPTIVE=GEOM SIGMA_MIN=0.001 SIGMA_MAX=0.1
 GRID_MIN=-0.05 GRID_MAX=0.55 GRID_BIN=250
 RESTART=YES
...
# Reweighting values and bias from Metadynamic simulations
rw: REWEIGHT_BIAS TEMP=300.0
hh: HISTOGRAM ARG=dd.* GRID_MIN=-0.05 GRID_MAX=0.55 GRID_BIN=250 BANDWIDTH=0.0003
CLEAR=2500 LOGWEIGHTS=rw
DUMPGRID GRID=hh FILE=my_histogram.dat STRIDE=2500
ENDPLUMED
```

Section S5.- Calculation of the thermal expansion coefficient, α, and the specific heat, Cp.

The thermal expansion, α, ðand the specific heat, *Cp*; were calculated according to the following expressions: $_{p}$

$$\alpha = \frac{1}{L_O}\left(\frac{\partial \mathrm{L}}{\partial \mathrm{T}}\right)_p \qquad \text{Equation S6}$$

where L_0 is the average length of the computational cell and *L* is the actual size at a given temperature (*T*).

$$C_p = \frac{1}{M}\left(\frac{\partial \mathrm{Q}}{\partial \mathrm{T}}\right)_p \qquad \text{Equation S7}$$

where *M* is the mass of the solid considered in the simulation cell and *Q* is enthalpy at a given temperature *T*.

Having the cell parameter and energy as functions of the temperature, the curved were numerically fitted to third order polynomials. Then, the fitted equations were differentiated with respect to temperature at to obtain α and *Cp*.

Section S6.- Calculation of mean-squared displacements of methanol and water Ag-CRI ST3 ONM

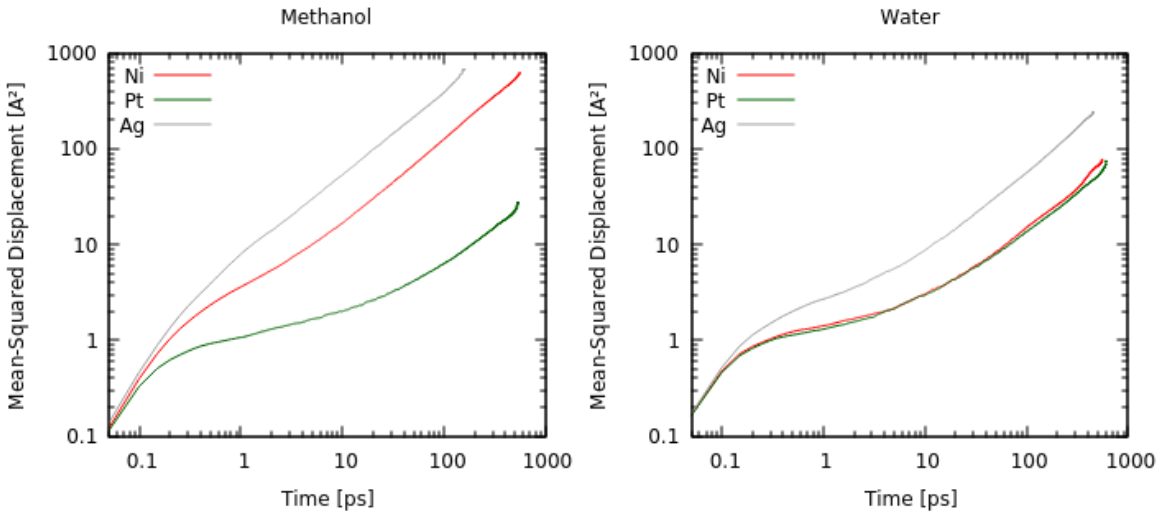

Figure S5. Mean-squared displacement of methanol and water in Ni-, Pt-, and Ag-CRI ST3 ONM, with which to calculate the diffusion coefficients. These results comes from our MD simulations.

Section S7.- List of stable ONMs structures designed in this work

The structures of our newly-designed, stable ONMs are given as separated CIFs files:

1. ONM_from_MOF_IRMOF16.cif
2. ONM_from_MOF_NDC-MIL101.cif
3. ONM_from_MOF_PCN6P.cif
4. ONM_from_ST_CRI-ST3.cif
5. ONM_from_ST_CRI-ST4.cif
6. ONM_from_ST_SOD-ST3.cif
7. ONM_from_ST_SOD-ST4.cif

Section S8.- Views of stable ONMs structures

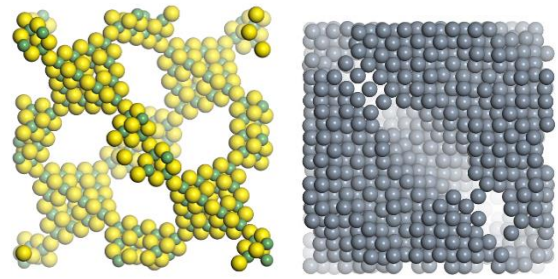

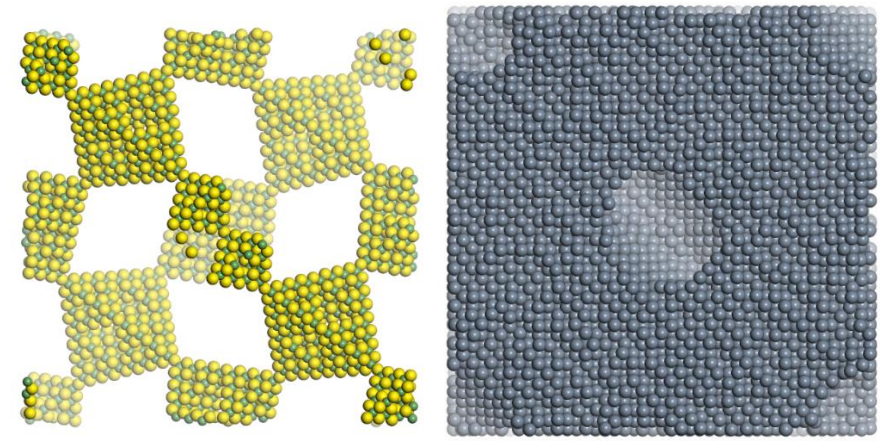

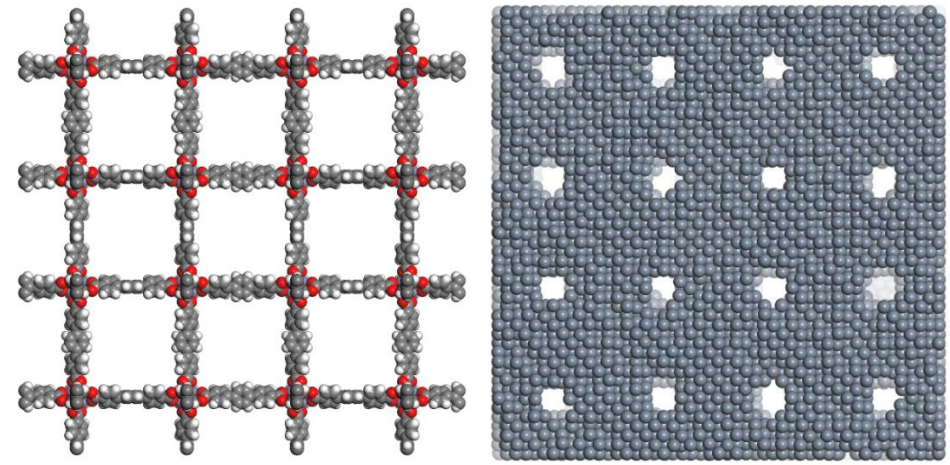

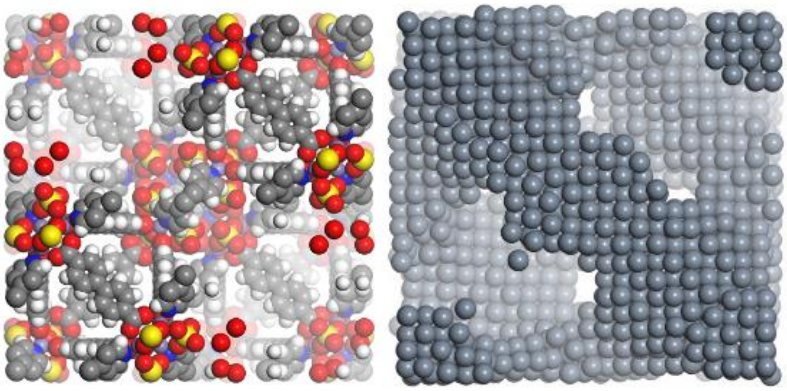

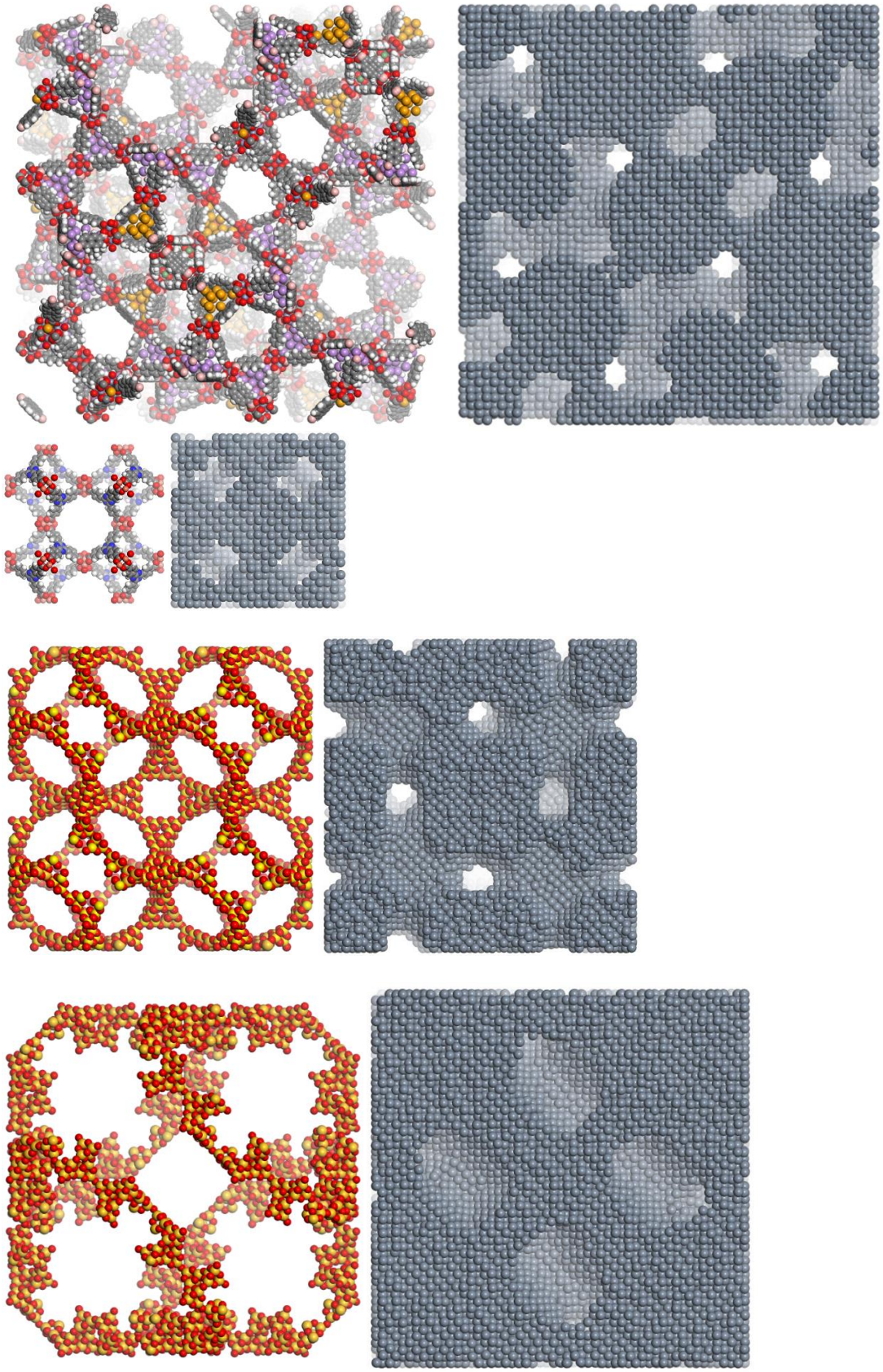

Figure S6. Templates (left) and OMMs (right) of the 8 predicted stable structures. From top to bottom: CRI-ST3, CRI-ST4, IRMOF16, MOF-500, NDC-MIL101, PCN-6P, SOD-ST3, SOD-ST4.

Section S9.- Energy per atom vs density for Ni and Pt ONMs with alternative potentials

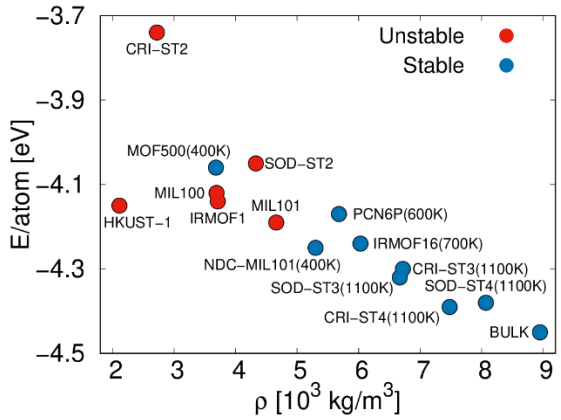

Figure S7a. Energy per atom vs density, for Ni ONMs. Stable structures, in blue, are accompanied by the highest temperature at which they are stable. Structures in red are not stable. Simulations were conducted here with Ortiz-Roldan et al. potentials.[S4]

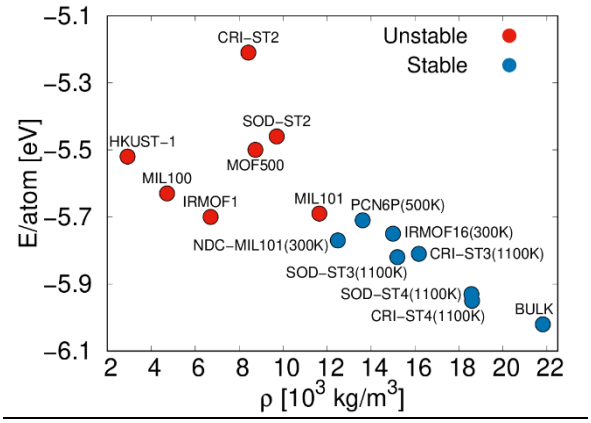

Figure S7b. Energy per atom vs density, for Pt ONMs. Stable structures, in blue, are accompanied by the highest temperature at which they are stable. Structures in red are not stable. Simulations were conducted here with Johnson potentials.[S5]

Section S10.- Porosities of stable ONMs

Table S1. Porosity of our stable ONMs: PLD (pore limiting diameter Å), LCD (large cavity diameter Å), AccHVF (accessible Helium void fraction), AccFreeVolFrac (accessible free volume fraction), AccSAVolum (accessible volumetric surface area m^2/cm^3).

ONM	PLD	LCD	AccHVF	AccFreeVolfrac	AccSAvolum
ONM_MOF_IRMOF16	5.71	9.85	0.228	0.291	786.22
ONM_MOF_NDC_MIL101	11.16	16.91	0.384	0.432	935.69
ONM_MOF_PCN6p	6.21	8.99	0.304	0.370	1082.30
ONM_ST_cri_GeS2_ST3	6.90	11.44	0.245	0.293	764.69
ONM_ST_cri_GeS2_ST4	6.83	15.01	0.111	0.130	292.21
ONM_ST_SOD_GeS2_ST3	6.04	10.42	0.190	0.229	635.85
ONM_ST_SOD_GeS2_ST4	6.16	12.83	0.113	0.141	351.92

Section S11.- Empirical formula for calculating the critical PLD of stable ONMs

The critical PLD of the template structure is obtained according to the following scheme:

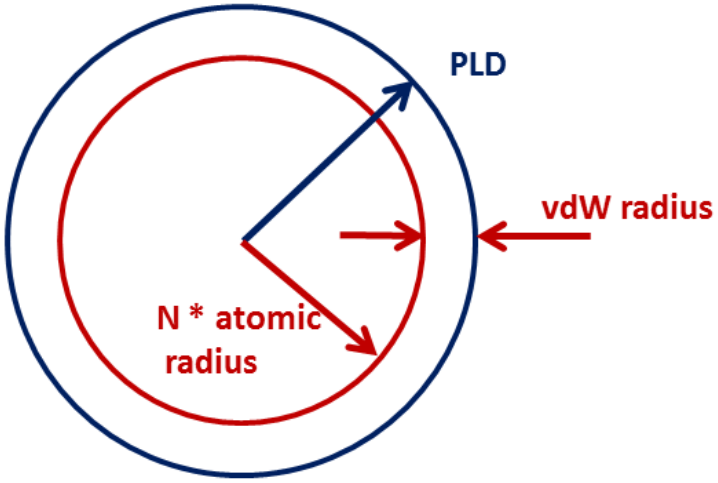

We can obtain a critical value of pore limiting diameter (PLDc) as the diameter below which a template structure will not give rise to a stable ONM. From the geometrical relations shown in the figure above, it is clear that: $PLDc = 2 \cdot R_{vdw} + N \cdot R_{atom}$. Given that the value of PLDc observed for Pt ONMs is ~15 Å, we get a value of N = 7.5 for Pt (which provides a Pt – Pt distance within 1 % of that obtained compared to experimentally for the Pt structure). From that value, we can introduce a general formula with which to predict the PLDc of potential template structures, as:

$$PLDc = 2 \cdot R_{vdw} + 7.5 \cdot R_{atom}$$

Section S12.- Porosities and stabilities of template MOFs and ST solids

Table S2. Porosities and stabilities of template MOFs and ST solids: Stability of corresponding ONM (unstable, medium stability, high stability), PLD (pore limiting diameter, Å), LCD (large cavity diameter, Å), AccHVF (accessible Helium void fraction), AccFreeVolFrac (accessible free volume fraction), AccSAVolum (accessible volumetric surface area, m^2/cm^3).

Solid	Stability	PLD	LCD	AccHVF	AccFreeVolfrac	AccSAvolum
MOF simulated						
MOF_HKUST	Unst.	6.37	12.74	0.685	0.634	1645.98
MOF_IRMOF1	Unst.	7.80	15.03	0.820	0.771	2047.65
MOF_IRMOF16	Med.	17.10	25.19	0.933	0.904	1245.96
MOF_MIL100	Unst.	8.61	26.38	0.680	0.653	1320.32
MOF_MIL101	Unst.	13.31	33.3	0.787	0.747	1154.75
MOF_NDC_MIL101	Med.	15.31	40.97	0.883	0.765	1028.82
MOF_MOF500	Unst.	10.12	19.56	0.762	0.714	1574.68
MOF_PCN6p	Med.	14.76	22.86	0.872	0.849	1499.37
Supertetrahedra simulated						
ST_cri_GeS2_ST2	Unst.	7.40	9.54	0.883	0.719	2039
ST_cri_GeS2_ST3	High	18.34	22.83	0.933	0.866	1057.49
ST_cri_GeS2_ST4	High	42.96	52.27	0.965	0.935	438.99
ST_SOD_GeS2_ST2	Unst.	7.58	18.17	0.895	0.765	1666.82
ST_SOD_GeS2_ST3	Med.	18.59	40.72	0.942	0.885	900.92
ST_SOD_GeS2_ST4	High	42.24	86.77	0.969	0.944	387.06
MOF experimental						
MOF_BUT12	High	16.94	23.93	0.799	0.759	1204.19
MOF_MOF808	High	10.80	17.77	0.716	0.698	1599.88
MOF_PCN777	High	28.17	33.52	0.894	0.882	729.84

Section S13.- Distribution of adsorption enthalpies and transport of benzene and xylene isomers

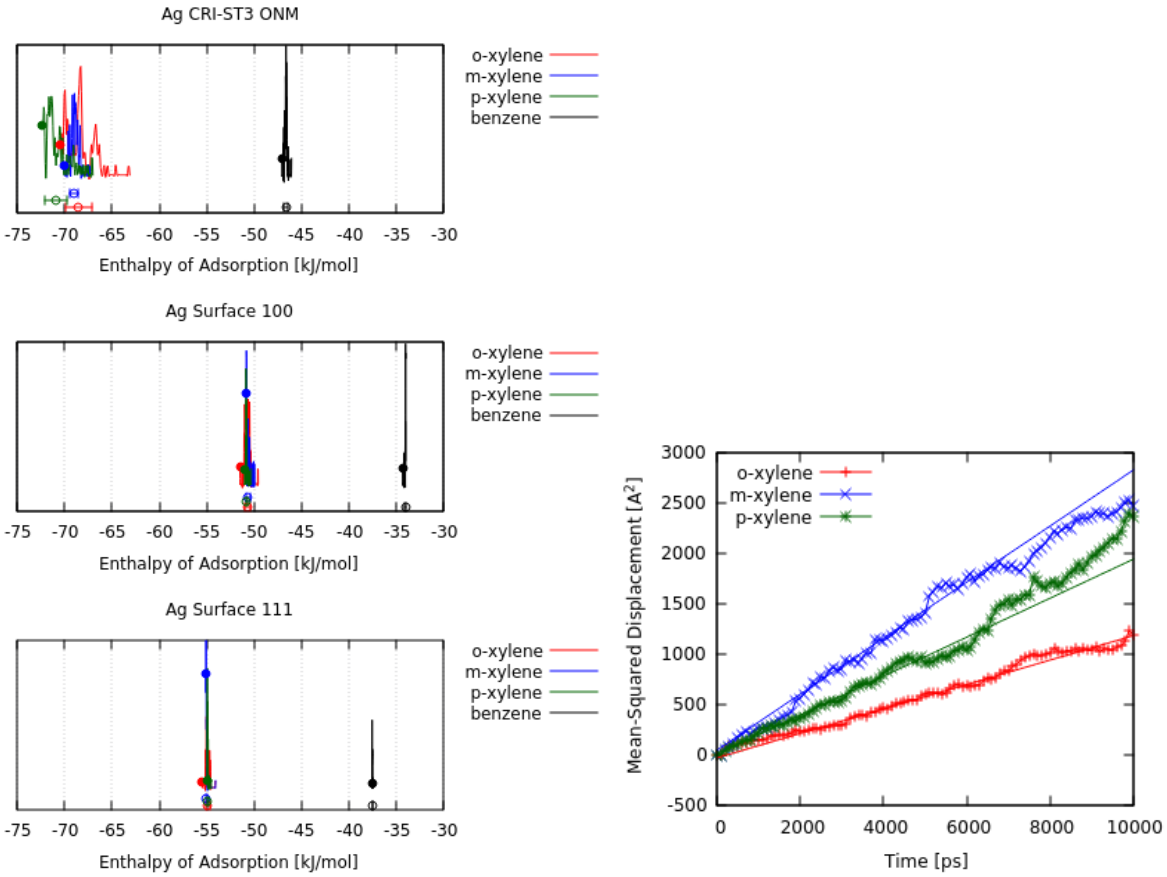

Figure S8. (Left) Distribution of enthalpies of adsorption, calculated by MC simulations at low coverage, for the xylene isomers and benzene in the Ag-CRI ST3 ONM, and 100- and 111-surfaces. **(Right)** Mean-squared displacement of the xylene isomers in the Ag-CRI-ST3 ONM in time.

Section S14.- References

S1- J. Li, X. Dai, S. Liang, K. Tai, Y. Kong and B. Liu, Physics Reports, 2008, 455, 1-134.

S2- Y. Mishin, M. Mehl and D. Papaconstantopoulos, Physical Review B, 2002, 65, 224114.

S3- H. W. Sheng, M. J. Kramer, A. Cadien, T. Fujita and M. W. Chen, Phys. Rev. B - Condens. Matter Mater. Phys., 2011, 83, 1–20.

S4- J. M. Ortiz-Roldan, A. R. Ruiz-Salvador, S. Calero, F. Montero-Chacón, E. García-Pérez, J. Segurado, I. Martin-Bragado and S. Hamad, Phys. Chem. Chem. Phys., 2015, 17, 15912–15920

S5- R. Johnson, Physical Review B, 1989, 39, 12554.

S6- A. Laio, M. Parrinello, Escaping free-energy minima, Proc. Natl. Acad. Sci. 99 (2002) 12562–12566.

S7- A. Barducci, G. Bussi, M. Parrinello, Well-Tempered Metadynamics: A Smoothly Converging and Tunable Free-Energy Method, Phys. Rev. Lett. 100 (2008) 20603.

S8- D.A. Colón-Ramos, P. La Riviere, H. Shroff, R. Oldenbourg, Transforming the development and dissemination of cutting-edge microscopy and computation, Nat. Methods. 16 (2019) 667–669.

S9- G.A. Tribello, M. Bonomi, D. Branduardi, C. Camilloni, G. Bussi, PLUMED 2: New feathers for an old bird, Comput. Phys. Commun. 185 (2014) 604–613.

S10- G.A. Tribello, F. Giberti, G.C. Sosso, M. Salvalaglio, M. Parrinello, Analyzing and Driving Cluster Formation in Atomistic Simulations, J. Chem. Theory Comput. 13 (2017) 1317–1327.